Catalysis Letters 36 (1996) 255–261

Synthesis of metal-incorporated mesoporous crystalline silicates for oligomerization of propene

Jin-Bae Kim and Tomoyuki Inui [1]

Division of Energy and Hydrocarbon Chemistry, Graduate School of Engineering, Kyoto University, Sakyo-ku, Kyoto 606-01, Japan

Received 23 February 1995; accepted 29 September 1995

Mesoporous crystalline silicates were synthesized with incorporation of various metal components such as Al, Ga, or Fe. Mesoporous silicate synthesized without metal incorporation showed the highest thermal stability. Although the thermal stability was weakened by metal incorporation, Al- and Fe-mesoporous-silicate with lower metal content (Si/metal atomic ratio of 200) maintained the high surface area about 600 m^2/g after the calcination at 1000°C for 0.5 h. Even when the same surfactant (dodecyltrimethylammonium bromide) was used as template, the pore diameter and wall thickness were changed by the gel mixture composition and the thermal stability of mesoporous silicates could be enhanced by increase in wall thickness. The catalytic activity of Al-mesoporous-silicate was also increased with an increase in pH of the gel mixture before crystallization. Although the catalytic activity of mesoporous silicate was lower than the activities of the other zeolitic catalysts like ZSM-5, a considerable amount of oligomers was produced from propene even at the lower temperature range and the possibility for the production of larger organic molecules could be confirmed.

Keywords: mesoporous crystalline silicate; metal incorporation; thermal stability; propene oligomerization

1. Introduction

Recently, a new family of mesoporous materials, denoted as MCM-41, was reported by researchers at Mobil Co. [1,2]. These materials could be synthesized hydrothermally in the presence of alkyltrimethylammonium surfactant cations. They possess a regular hexagonal array of a uniform channel size ranging between 20 and 100 Å. Independently, Inagaki et al. [3,4] synthesized a similar mesoporous material having a channel size of about 40 Å by ion-exchange treatment of kanemite [5] with an aqueous solution of hexadecyltrimethylammonium chloride. These new mesoporous materials are expected to be useful as the catalysts for reactions of high molecular weight hydrocarbons because of lower diffusion resistance due to their large pore diameters. Recently, ultra-large pore zeolites such as VPI-5 [6–8], cloverite [9–11], and JDF-20 [12,13] have been synthesized; however, these materials have not been applied to catalysts, maybe owing to their structural instabilities. On the other hand, mesoporous materials possess much higher thermal stability than the above-mentioned ultralarge pore zeolites, and furthermore, the pore size can be controlled according to the length of the alkyl side chain in the surfactant.

Concerning the application of the newly developed mesoporous crystalline silicate, we have already reported [14] that the mesoporous silicate synthesized by ion-exchange treatment from kanemite showed a high performance for hydrogenation of alkenes in the gasoline range as a catalyst support especially under higher flow rate conditions. The synthesis of the mesoporous silicate from kanemite has some advantages, such as the lower concentration of surfactant and shorter crystallization time compared with those of MCM-41 [4], although, in the case of metal incorporation, it has to be conducted after the crystallization [3]. By contrast, for the synthesis of metal-incorporated MCM-41s, various metal components can be introduced at the stage of gel formation before hydrothermal treatment for the crystallization. In practice, metal incorporation such as Al [15–17] and Ti [18,19] into the framework of MCM-41 was reported; however, their property and catalytic activity have not been studied sufficiently.

In this study, in order to promote the catalytic property, incorporation of various metal ions such as Al, Ga, or Fe into the framework of mesoporous silicate were investigated by adopting the method of Mobil Co. [1]. The optimum conditions for the synthesis of mesoporous silicate and the effect of various synthesis conditions on the properties of mesoporous crystalline silicates were studied in detail. The thermal stability of various mesoporous silicates synthesized in this study was estimated by raising the calcination temperature, and the catalytic performance of those samples were investigated through the oligomerization of propene as the model reaction.

2. Experimental

2.1. Catalyst preparation

The synthesis of mesoporous silicate materials was

---

[1] To whom correspondence should be addressed.

based on the preparation procedure of MCM-41 [1]. The surfactants used in the early stage of MCM-41 synthesis were alkyltrimethylammonium bromide and/or chloride with alkyl groups $C_{12}H_{25}$, $C_{14}H_{29}$, and $C_{16}H_{33}$. The incorporation of various metals into the mesoporous silicate structure was carried out by employing dodecyltrimethylammonium bromide (DDTMABr) which resulted in the formation of mesoporous silicate with the highest crystallinity. A sodium silicate solution (water glass) was mainly used as the silicon source, although Aerosil (Nippon Aerosil Co. Ltd.) and Cataloid-30 (Shokubai Kasei Co. Ltd.) were also examined for the synthesis of mesoporous silicate.

The starting mixtures for synthesis were prepared using water glass (Koso), DDTMABr (Tokyo Kasei), sulfuric acid (Wako). Aluminium nitrate (Wako), gallium sulfate (Mitsuwa), and iron nitrate (Wako) were used as the sources of Al, Ga, and Fe, respectively. A 30 g portion of water glass (29% SiO_2) and 60 g of water were mixed while stirring. After stirring for about 10 min, the metal source and sulfuric acid were slowly added. The 25% surfactant solution was then added to the mixture, and the resulting gel was allowed to stir for 30 min. A prescribed amount of water was then added to the gel. A base composition of the gel mixture was $SiO_2 : 0.33Na_2O : 0.5DDTMABr : 0.149H_2SO_4 : 68.3H_2O$, and the ratios of H_2O/SiO_2, H_2SO_4/SiO_2, and Si/metal were varied in the range of 56.8–92.9, 0.062–0.149, and 50–200, respectively. The resulting gel was heated at 150°C in an autoclave for 65 h. The resulting solid products were washed with distilled water by using a centrifuge. The crystals were then dried, and treated in an air stream at 540°C for 6 h to burn off the surfactant and to calcine. The calcined crystals were made into tablets and crushed to 10–20 mesh to be used as the catalysts for the reaction.

2.2. *Catalyst characterization*

Powder X-ray diffraction (XRD) analysis was carried out on a Shimadzu XD-D1 with nickel filtered Cu Kα radiation at a scanning speed of 1°/min. Pore size distribution curves were calculated from the nitrogen adsorption isotherms measured on a Shimadzu Micromeritics AccuSorb 2100E at 77.4 K with the constant volume method. BET surface areas of the calcined samples were measured by nitrogen gas adsorption with the continuous flow method using a gas chromatograph at liquid nitrogen temperature and helium flow as the carrier gas.

2.3. *Reaction method*

The propene-conversion reaction was carried out by using an ordinary flow-type reactor [20] operating under atmospheric pressure. A 0.6 g (ca. 1.5 ml) portion of the catalyst was packed in a quartz tubular reactor of 8 mm inner diameter, and then it was pretreated with a nitrogen flow at 500°C for 30 min to standardize the catalyst surface state by removal of the pre-adsorbed water. Non-diluted propene was introduced under the gaseous hourly space velocity (GHSV) of 500 h^{-1}. The reaction was carried out at a temperature range from 150 to 400°C. The products were analyzed by using three gas chromatographs equipped with integrators. MS-5A, VZ-10 and Silicon-OV-101 columns were used to analyze hydrogen and the whole range of hydrocarbons produced.

3. Results and discussion

3.1. *Synthesis of various metal-incorporated mesoporous silicates*

Figs. 1 and 2 show the XRD patterns and BET surface areas of various mesoporous silicates calcined at 540°C for 6 h and at 1000°C for 0.5 h, respectively. Each as-synthesized sample shows evident XRD patterns similar to that of MCM-41 [1], although the spacing of the crystal surface was reduced to some extent by the metal incorporation. This result indicates that added metal components could be incorporated in the crystal domain with a high dispersion state. The values of XRD d_{100}-spacing of the as-synthesized mesoporous silicates were reduced about 2–5 Å by calcination at 540°C, and further reductions of about 5–7 Å were observed by calcination at 1000°C for 0.5 h. Mesoporous silicate without metal incorporation (non-metal mesoporous

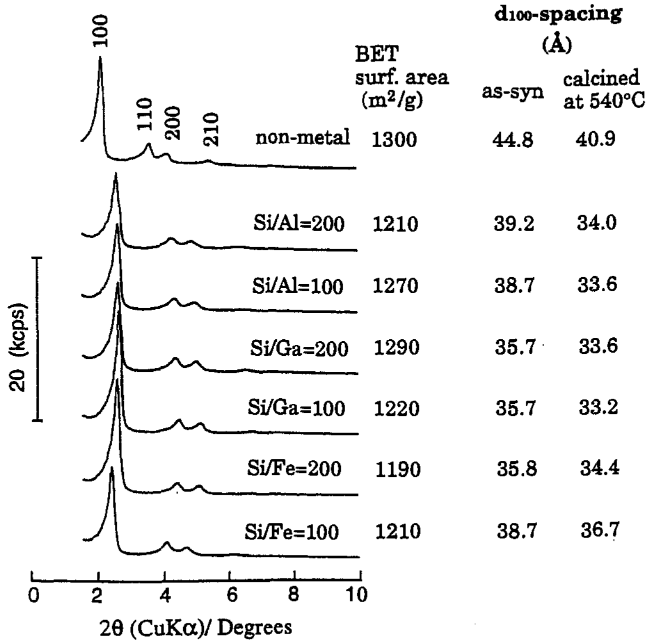

Fig. 1. X-ray diffraction patterns and BET surface areas of various mesoporous silicates calcined at 540°C for 6 h. Si/metal atomic ratio is the charged one.

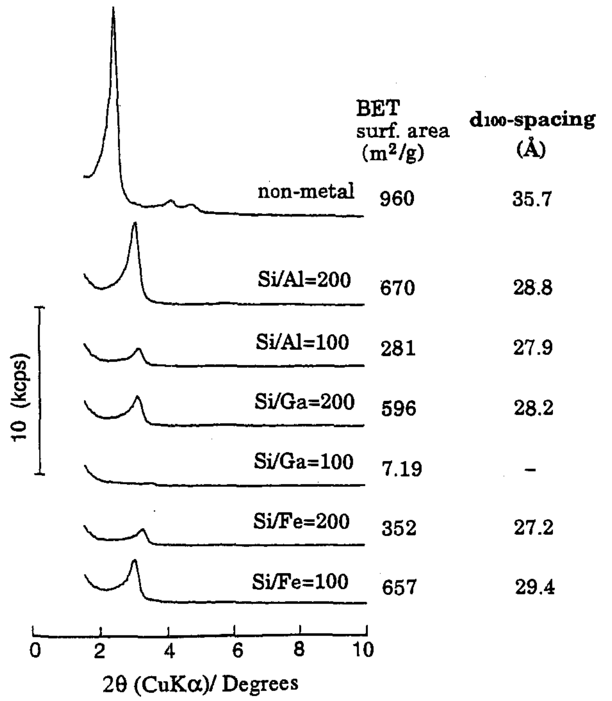

Fig. 2. X-ray diffraction patterns and BET surface areas of various mesoporous silicates calcined at 1000°C for 0.5 h. Si/metal atomic ratio is the charged one.

silicate) showed the largest value of XRD d_{100}-spacing and the highest BET surface area of 1300 m^2/g. As shown in fig. 2, the XRD pattern and high surface area of non-metal mesoporous silicate were maintained even after the calcination at 1000°C for 0.5 h, indicating that the thermal stability was higher than that of various metal-incorporated mesoporous silicates. The thermal stability was lowered by the metal incorporation. Moreover, the higher metal content in metal-incorporated mesoporous silicates showed the lower stability except for the Fe-mesoporous-silicate. From the comparison between figs. 1 and 2, the higher thermal stability was generally obtained from the sample having the larger d_{100}-spacing.

Since the base composition of mixture gels for the synthesis of mesoporous silicates shown in figs. 1 and 2 was carefully maintained as described in the experimental section, except that the amount of water slightly varied in the range of about 10%, the reason for the change in the d_{100}-spacing would be the change in gel composition by the addition of metal components. The effects of the amount of water and sulfuric acid (pH) on the crystallization of mesoporous silicate were then investigated in the case of Al-incorporation as an example, and the results are shown in figs. 3 and 4, respectively. The d_{100}-spacing value and thermal stability decreased with increase in the amount of water, as shown in fig. 3. Not only the pore size but also the thickness of the wall of mesoporous silicate was considered as the reason of variation of d_{100}-spacing. Although the pore size might be changed by various crystallization conditions, the higher thermal stability of the mesoporous silicate synthesized with the smaller amount of water would be due to the thicker wall. As shown in fig. 4, a similar result was obtained from the effect of pH which was controlled by the amount of sulfuric acid added to the gel mixture before crystallization. When the smaller amount of sulfuric acid was mixed with the gel mixture, i.e., under the condition of higher pH, the higher crystallinity and thermal stability of mesoporous silicate were obtained. However, the crystallinity of mesoporous silicate synthesized without sulfuric acid, i. e., too high pH, was very low, and the XRD peaks hardly remained after calcination.

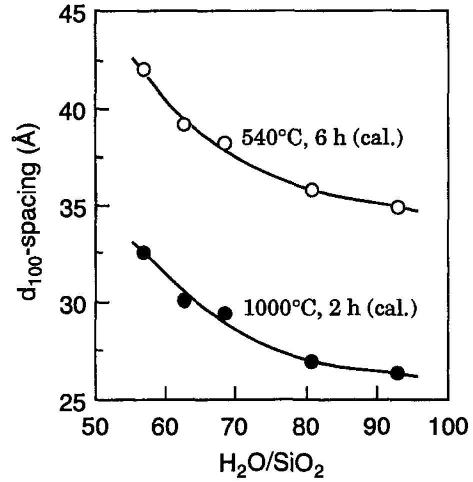

Fig. 3. Effect of water content in the gel mixture on the crystallization of Al-mesoporous-silicate (Si/Al = 100).

Table 1 shows the BET surface area and the wall thickness estimated from the nitrogen-adsorption data and d_{100}-spacing of the Al-mesoporous-silicate crystallized with a different water content in the gel mixture. The pore diameter was reduced and the pore size distribution curve was broadened by increase of the water content in the gel mixture. This result indicates that the

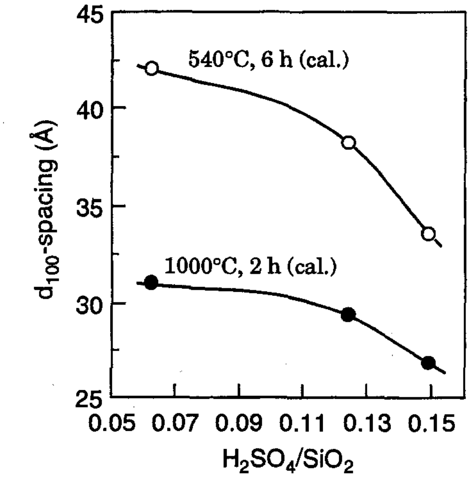

Fig. 4. Effect of pH on the crystallization of Al-mesoporous-silicate (Si/Al = 100).

Table 1
Physical properties of Al-incorporated mesoporous silicates shown in fig. 3

H_2O/SiO_2 [a]	BET surf. area [b] (m^2/g)	Pore diameter (Å)	d_{100}-spacing (Å)	a_0[c](Å)	Wall thickness [d](Å)
56.8	932	32.8	42.1	48.6	15.8
68.3	1020	30.5	38.2	44.1	13.6
92.9	1070	27.7	34.9	40.3	12.6

[a] Water content in the gel mixture as shown in fig. 5.
[b] Calculated from the data of nitrogen adsorption isotherm.
[c] Repeat distance including the pore wall ($2d_{100}/\sqrt{3}$).
[d] Calculated from the values of a_0 and pore diameter.

mesoporous silicate with a more uniform channel size can be synthesized through adjustment of composition in the gel mixture. Since the same surfactant was employed as the template for the crystallization of mesoporous silicates, the variation of pore size with the water content might be due to a change in the surfactant micelle (maybe surfactant concentration in the micelle) before the formation of silicate framework. The estimated wall thickness also changed with the water content. Consequently, the mesoporous silicate synthesized with the smaller amount of water showed the lower surface area and the thicker pore wall. Although the change of wall thickness and pore size by pH and water content in the gel mixture and the thermal stability were similar to those given in ref. [20], the effect of pH on the pore spacing has yielded the opposite result. In the present preparation procedure, the silicate framework was more rapidly grown on the surfactant micelles under the conditions of moderately higher pH and lower water content.

3.2. Oligomerization of propene on various mesoporous silicates

Fig. 5 shows the change in propene conversion with increase of time on stream on the Fe-mesoporous-silicates (Fe-mesoporous-silicate) having different iron content, and the results are compared with that of non-metal mesoporous silicate. On the Fe-mesoporous-silicate with Si/Fe ratio of 200, the propene conversion was about twice that on the non-metal mesoporous silicate. The enhancement of catalytic activity by introducing a small amount of iron suggests that the iron ingredient was effectively incorporated in the silicate framework. However, the Fe-mesoporous-silicates with higher iron content (Si/Fe ratios of 100 and 50) showed lower activities than the non-metal one. Since the non-metal mesoporous silicate modified with iron by impregnation showed a similar result to the Fe-mesoporous-silicates with Si/Fe ratios of 100 and 50, an increase of non-framework iron species resulted in a lowering of catalytic activity. The change in product distribution of propene conversion on Fe-mesoporous-silicate (Si/Fe = 200) with increase of time on stream is shown in table 2. The product mainly consisted of dimers and trimers of propene. The high molecular weight hydrocarbons with carbon number above 15 could be detected in the initial products. The Fe-mesoporous-silicate markedly deactivated with increase in time on stream. Since the aromatics were hardly produced, the deactiva-

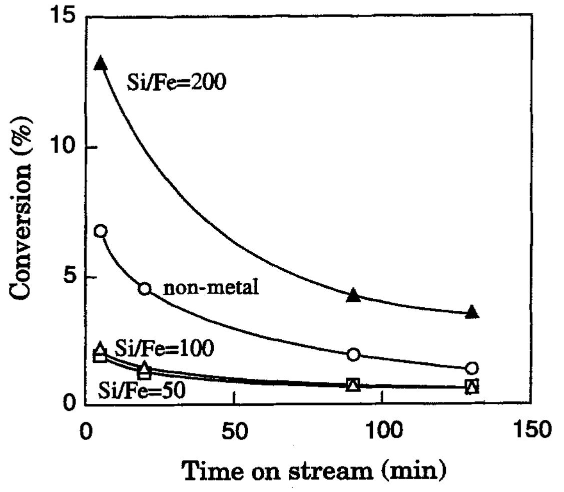

Fig. 5. Change in propene conversion on Fe-mesoporous-silicates having different Si/Fe ratios with increase in time on stream. Reaction temperature = 300°C, GHSV = 500 h^{1-}.

Table 2
Change in product distribution of propene conversion on Fe-mesoporous-silicate (Si/Fe = 200) with increase of time on stream at 300°C, and propene GHSV = 500 h^{-1}

	Time on stream (min)		
	5	90	130
conversion (%)	12.7	4.27	3.58
selectivity (wt%)			
C_1–C_3	1.02	1.61	2.18
C_4	0.04	0.05	0.05
$C_4^=$	2.03	2.44	2.19
C_5	0.08	0.26	0.30
$C_5^=$	11.38	8.67	8.43
C_6	7.48	8.49	8.63
$C_6^=$	65.91	74.55	74.81
C_7	2.36	0.32	0.17
C_8	2.71	1.19	0.71
C_9	6.55	2.41	2.52
C_{10+}	0.44	trace	trace
aromatics	trace	trace	trace

tion might be due to formation of olefinic coke inside the large pores.

Fig. 6 shows the change in propene conversion at various reaction temperatures ranging from 150 to 400°C on the Fe-mesoporous-silicate with Si/Fe ratio of 200, which showed the highest activity, as shown in fig. 5. The propene conversion increased with increase in temperature up to 300°C. The decrease of propene conversion at 400°C is considered to be caused by the reproducing of propene by cracking of oligomers. In practice, the selectivity to light alkenes in the range of C_2–C_4 at 400°C was higher than that at the lower temperature range. Even at the very low temperature range, such as 150 and 200°C, the propene fed was considerably converted to higher hydrocarbons. On the MFI-type zeolite catalysts, such as H-ZSM-5 and H-Fe-silicate [21], the conversion of light alkenes proceeded above 250°C under the same reaction conditions. On the other hand, it was reported [22] that the light alkenes adsorbed inside the pores of ZSM-5 could be converted to oligomer and/or polymer even at room temperature. Since the mesoporous silicates have almost no spatial restrictions, the oligomer produced at the lower temperature range could be easily removed from the inside of pores. Thus the mesoporous silicates possessing lower activity showed higher propene conversion than the MFI-type zeolites only at the lower temperature range.

Fig. 7 shows the results of propene-conversion reaction on Al- and Ga-mesoporous-silicates under the same reaction conditions as in fig. 5. The Al-mesoporous-silicate with Si/Al ratio of 200 showed the highest catalytic activity. It was similar to the Fe-mesoporous-silicates in that the conversion of propene was smaller on the Al-mesoporous-silicate with higher aluminium content (Si/Al ratio of 100). The propene conversion on the Ga-mesoporous-silicate was higher than the Fe-mesoporous-silicate and lower than the Al-mesoporous-silicate. Product distributions of propene conversion on Al-, Ga-, and Fe-mesoporous-silicates (Si/metal = 200) at time on stream of 5 min are shown in fig. 8. Although the aromatics were produced, with a selectivity of 2–3 wt%, on the Al- and Ga-mesoporous-silicates, the product mostly consisted of alkenes in the gasoline range. On the Al-mesoporous-silicate, selectivity to paraffins slightly increased with increase in selectivity to aromatics, which was similar to the result on the MFI-type H-Al-silicate (H-ZSM-5) [23,24]. Since the silicate framework of the mesoporous silicate exhibits an irregular molecular arrangement, the acidity and the catalytic activity of metal-incorporated mesoporous silicates were lower than those of the MFI-type metallosilicates. However, a considerable effect of the various metals incorporated in the mesoporous silicate on the catalytic activity for the oligomerization of propene was confirmed.

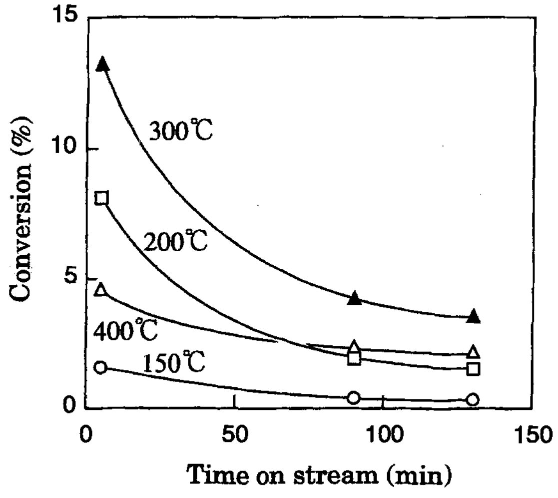

Fig. 6. Change in propene conversion on Fe-mesoporous-silicate with Si/Fe ratio of 200 with increase in time on stream at various reaction temperatures. GHSV = 500 h^{-1}.

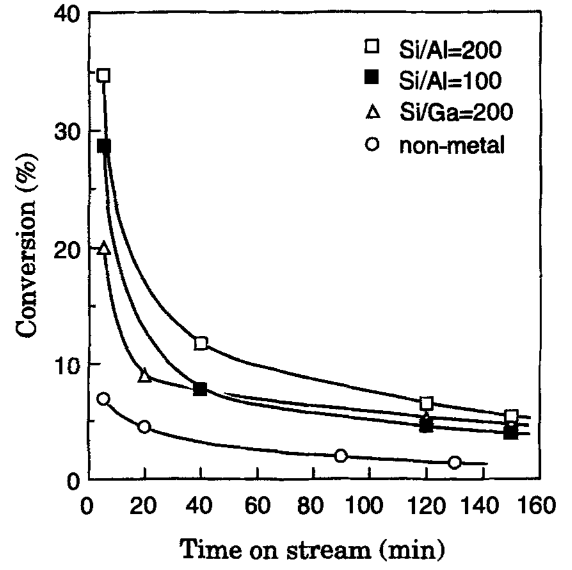

Fig. 7. Change in propene conversion on Al- and Ga-mesoporous-silicates with increase in time on stream. Reaction temperature = 300°C, GHSV = 500 h^{-1}.

The metal-incorporated mesoporous silicates used for the propene conversion in figs. 5–8 were synthesized from the gel mixture of the base composition described

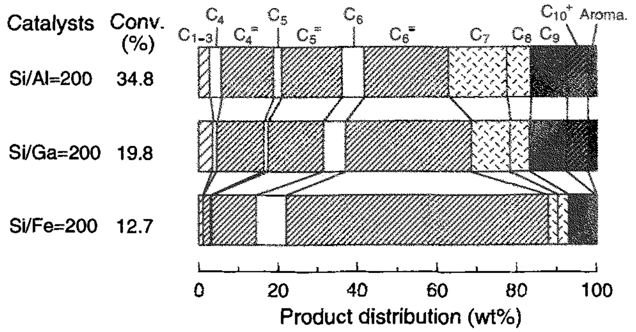

Fig. 8. Product distribution of propene conversion on Al-, Ga-, and Fe-mesoporous-silicates (Si/metal = 200). Reaction temperature = 300°C, GHSV = 500 h^{-1}, time on stream = 5 min.

in the experimental section with the addition of various metal sources. For the metal-incorporated mesoporous silicates synthesized from the base gel composition, the catalytic activity for the oligomerization of propene could not be enhanced by the introduction of higher amounts of metal components than that of Si/metal charged ratio of 200. The propene-conversion reactions were conducted on the Al-mesoporous-silicates with Si/Al ratio of 100 synthesized from the gel mixture with various compositions (figs. 3 and 4). On the Al-mesoporous-silicates synthesized under the conditions of different water content in the gel mixture, the conversions of propene for time on stream of 5 min were varied in the range of 42–48% independently of the change in water content. Fig. 9 shows the effect of pH of the gel mixture on the catalytic activity of Al-mesoporous-silicates. The Al-mesoporous-silicate with Si/Al charged ratio of 100 synthesized with an addition of higher amount of H_2SO_4 (pH of gel mixture was 11.2) showed a slightly lower propene conversion than the Si/Al ratio of 200 (fig. 7), although the observed aluminium contents agreed with the charged values. However, the catalytic activity on the Al-mesoporous-silicate with Si/Al ratio of 100 markedly increased with an increase in pH of the gel mixture. On the other hand, propene conversion on the Al-impregnated silica gel with Si/Al ratio of 100, employed as a reference catalyst, was also compared with that on the Al-mesoporous-silicates in fig. 9. The decrease in propene conversion with time on stream on the Al-mesoporous-silicate was larger than that on the Al-impregnated silica gel. The one-dimensional straight channel of mesoporous silicate might be responsible for the fast deactivation. However, the Al-mesoporous-silicate synthesized with the addition of lower amount of H_2SO_4 (pH of gel mixture was 11.9) showed a higher initial activity in propene conversion than the Al-impregnated silica gel. These results indicated that the remarkably high surface area of mesoporous silicate and the more effective incorporation of aluminium by increasing the pH of the gel mixture could contribute to the enhancement of catalyst performance.

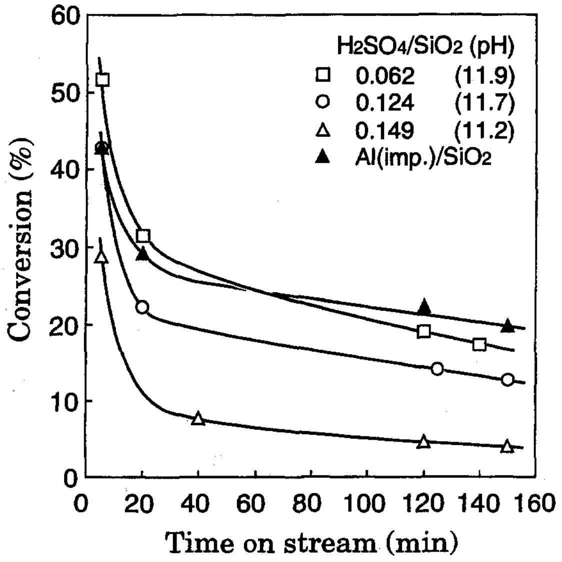

Fig. 9. Change in propene conversion on Al-mesoporous-silicates synthesized under the different pH condition as shown in fig. 4 and Al-impregnated silica gel with increase in time on stream. Reaction temperature = 300°C, GHSV = 500 h^{-1}.

4. Conclusions

Various metal-incorporated mesoporous silicates could be synthesized and they showed high crystallinity and surface area above 1000 m^2/g. The non-metal mesoporous silicate showed the highest thermal stability. Although the thermal stability weakened by metal incorporation, Al- and Fe-mesoporous-silicate with lower metal content maintained the high surface area of about 600 m^2/g after calcination at 1000°C for 0.5 h. The d_{100}-spacing in the XRD pattern and the thickness of the wall of mesoporous silicate were changed by various conditions, such as the amount of water, pH of the mixture gel, and addition of various metal components. The thermal stability generally increased with increase in the d_{100}-spacing. Since the atomic arrangement in the framework of mesoporous silicate was irregular like amorphous silica, the catalytic activity of mesoporous silicate was lower than the activities of the zeolitic catalysts, such as MFI-type metallosilicates [23,24]. However, a considerable amount of oligomers was produced from propene even at the lower temperature range, which was owing to little restrictions by the pore size of those mesoporous silicates. The possibility for the synthesis of larger molecules could be confirmed.

References

[1] J.S. Beck, J.C. Vartuli, W.J. Roth, M.E. Leonowicz, C.T. Kresge, K.D. Schmitt, C.T.-W. Chu, D.H. Olson, E.W. Sheppard, S.B. McCullen, J.B. Higgins and J.L. Schlenker, J. Am. Chem. Soc. 114 (1992) 10834.

[2] C.T. Kresge, M.E. Leonowicz, W.J. Roth, J.C. Vartuli and J.S. Beck, Nature 359 (1992) 710.

[3] S. Inagaki, Y. Fukushima, A. Okada, T. Kurauchi, K. Kuroda and C. Kato, in: *Proc. 9th Int. Zeolite Conf.*, Vol. 1, eds. R. von Ballmoos, J.B. Higgins and M.M.J. Treacy (Butterworth-Heinemann, Boston, 1992) p. 305.

[4] S. Inagaki, Y. Fukushima and K. Kuroda, J. Chem. Soc. Chem. Commun. (1993) 680.

[5] K. Beneke and G. Lagaly, Am. Mineral. 62 (1977) 763.

[6] M.E. Davis, C. Saldarriga, C. Montes, J. Garces and C. Crowder, Nature 331 (1988) 698.

[7] B. Duncan, R. Szostak, K. Sorby and J.G. Ulan, Catal. Lett. 7 (1990) 367.

[8] M.E. Davis, C. Montes, P.E. Hathaway and J.M. Garces, in: *Zeolites: Facts, Figures, Future,* Studies in Surface Science and Catalysis, Vol. 49A (Elsevier, Amsterdam, 1989) p. 199.

[9] M. Estermann, L.B. McCusker, Ch. Baerlocher, A. Merrouche and H. Kessler, Nature 352 (1991) 320.

[10] A. Merrouche, J. Patarin, H. Kessler, M. Soulard, L. Delmotte, J.L. Guth and J.F. Jolly, Zeolites 12 (1992) 226.

[11] J.L. Guth, H. Kessler, P. Caullet, J. Hazm, A. Merrouche and J. Patarin, in: *Proc. 9th Int. Zeolite Conf.*, Vol. 1, eds. R. von Ballmoos, J.B. Higgins and M.M.J. Treacy (Butterworth–Heinemann, Boston, 1992) p. 215.

[12] Q. Huo, R. Xu, S. Li, Z. Ma, J.M. Thomas, R.H. Jones and A.M. Chippindale, J. Chem. Soc. Chem. Commun. (1992) 875.

[13] Q. Huo, R. Xu, S. Li, Y. Xu, Z. Ma, Y. Yue and L. Li, in: *Proc. 9th Int. Zeolite Conf.*, Vol. 1, eds. R. von Ballmoos, J.B. Higgins and M.M.J. Treacy (Butterworth–Heinemann, Boston, 1992) p. 279.

[14] T. Inui, J.-B. Kim and M. Seno, Catal. Lett. 29 (1994) 271.

[15] A. Corma, V. Fornés, M.T. Navarro and J. Pérez-Pariente, J. Catal. 148 (1994) 569.

[16] R. Schmidt, D. Akporiaye, M. Stöcker and O.H. Ellestad, in: *Zeolites and Related Microporous Materials: State of the Art 1994*, Studies in Surface Science and Catalysis, Vol. 84A (Elsevier, Amsterdam, 1994) p. 61.

[17] M. Janicke, D. Kumar, G.D. Stucky and B.F. Chmelka, in: *Zeolites and Related Microporous Materials: State of the Art 1994*, Studies in Surface Science and Catalysis, Vol. 84A (Elsevier, Amsterdam, 1994) p. 243.

[18] A. Corma, M.T. Navarro and J. Pérez-Pariente, J. Chem. Soc. Chem. Commun. (1994) 147.

[19] O. Franke, J. Rathousky, G. Schulz-Ekloff, J. Stárek and A. Zukal, in: *Zeolites and Related Microporous Materials: State of the Art 1994*, Studies in Surface Science and Catalysis, Vol. 84A (Elsevier, Amsterdam, 1994) p. 77.

[20] N. Coustel, F. Di Renzo and F. Fajula, J. Chem. Soc. Chem. Commun. (1994) 967.

[21] T. Inui, F. Okazumi, J. Tarumoto, O. Yamase, H. Matsuda, H. Nagata, N. Daito and A. Miyamoto, J. Japan. Petrol. Inst. 30 (1987) 249.

[22] T.J. Gricus Kofke and R.J. Gorte, J. Catal. 115 (1989) 233.

[23] T. Inui, O. Yamase, K. Fukuda, A. Itoh, J. Tarumoto, N. Morinaga, T. Hagiwara and Y. Takegami, in: *Proc. 8th Int. Congr. on Catalysis*, Vol. 3, Berlin, 2 July 1984 (Verlag-Chemie, Weinheim, 1984) p. 569.

[24] T. Inui, in: *Successful Design of Catalysts*, Studies in Surface Science and Catalysis, Vol. 44 (Elsevier, Amsterdam, 1989) p. 189.